NATIONAL ADVISORY COMMITTEE FOR AERONAUTICS

TECHNICAL MEMORANDUM

No. 1194

FORCE- AND PRESSURE-DISTRIBUTION MEASUREMENTS ON EIGHT FUSELAGES

By G. Lange

Translation of ZWB Forschungsbericht Nr. 1516, October 1941

Washington
October 1948

NATIONAL ADVISORY COMMITTEE FOR AERONAUTICS

TECHNICAL MEMORANDUM NO. 1194

FORCE- AND PRESSURE-DISTRIBUTION MEASUREMENTS ON EIGHT FUSELAGES*

By G. Lange

SUMMARY

The present report deals with force- and pressure-distribution measurements on a number of fuselage forms of varying slenderness ratio, varying rearward position of maximum thickness, and varying nose ratio. The effect of these parameters on the force and moment coefficients was determined. The linearity of the difference between the theoretical and experimental fuselage moments with the friction lift made it possible to indicate a neutral point and its travel with the different parameters. The pressure-distribution measurements yielded absolute values for the increase of velocity. A comparison with the theory indicated good agreement at small angles of attack, but considerable differences at greater angles of attack, where potential flow could no longer be assumed.

INTRODUCTION

The fuselages were designed as bodies of revolution, the meridian lines of which were derived from the curve ABC of figure 1(a). This curve consists of a quarter-circle AB and a parabola BC, the axis of which is OB (the transition of the two curves is continuous up to the third order). Using the line AD as axis provides the maximum thickness at 41 percent chord. Using an inclined axis, as EC, through the center of the circle places the maximum thickness farther forward, although the curve is no longer a circular arc back to the position of maximum thickness. For greater rearward positions of the maximum thickness, parabolas of the fourth degree are added as indicated in the figure, for which, again, the circular arc forms the forward part back to the position of maximum thickness.

---

*"Kraftmessungen und Druckverteilungsmessungen an 8 Rümpfen," Zentrale für wissenschaftliches Berichtswesen der Luftfahrtforschung des Generalluftzeugmeisters (ZWB), Berlin-Adlershof, Forschungsbericht Nr. 1516, Oct. 24, 1941.

The meridian curves for desired thickness ratios are obtained by compressing by a proportionality factor from the basic contours. The meridian curves so derived have a nondimensional nose radius $\frac{\rho/t}{(d/t)^2}$, that is independent of the thickness ratio and simply a function of the rearward position of the thickness. To make the shape of the nose independent of the rearward position and thickness ratio, that is, modify the normalizod nose radius by a multiple (2 × normal, 3 × normal) the ordinate values of the above meridian lines are multiplied by a thickening function that varies the ordinates at the nose substantially (flattening).

Altogether eight fuselage forms were involved, three of which show the variation of ono parameter while the other two are constant. Another fuselage has a curved mean line as partial experiment for a wing-nacelle combination to be measured later. The measured fuselages are reproduced in figure 1. The data for the individual parameters are given in tables I and II. All fuselages were 800 millimeters in length. They were made of improved wood. The surface was given a high polish.

The pressure-distribution test stations, 29 altogether, lie on a meridian line. The pressure was conducted by means of brass tubes in the fuselage toward the rear end and connected by isoplastic hose to a multiple manometer. The fuselage zone disturbed by the hose is measured by a static survey apparatus. For the suspension of the fuselages at the wind-tunnel balance a round rod at one fourth of the length from the tip was attached normal to the test meridian section. The rotation for the angle-of-attack setting was effectod in the plane of the meridian section in symmetrical air flow. For yawed flow of the test section at angle of attack $\alpha = 0$ the fuselage is turned about a wind axis that lies in the plane of the test section. This way the pressures at four points of the circumference are measured with one section.

The tests were run in the 1.2-meter tunnel of the DVL. The airspeed was 56.5 meters per second; the relatod Reynolds number is $Re = 3.1 \times 10^6$.

INTERPRETATION

The forces and moments from the three-component measurements were represented nondimensionally, the lift and drag coefficients in terms of volume$^{2/3}$ and the moment in terms of volume.

$$c_a = \frac{A}{qV^{2/3}} = f(\alpha)$$

$$c_w = \frac{W}{qV^{2/3}} = f(\alpha)$$

$$c_m = \frac{M}{qV} = f(\alpha)$$

No jet correction was applied.

The fuselage center line is the reference line for angle of attack α and angle of yaw β. For fuselage 8 - curved mean line - the axis of the axially symmetrical forebody is applicable. The reference point for the moments lies at one fourth of the fuselage length behind the nose. Tail-heavy moments are positive. The pressures p referred to dynamic pressure q are plotted against the fuselage center line.

The theoretical moments are computed according to Vandrey (FB 1093). It is

$$M = qf\left(\frac{d_{max}}{l}\right) \sin 2\alpha \frac{\pi}{4} \int_0^l d^2 \, dx$$

$f\left(\frac{d_{max}}{l}\right)$ is a form factor which with the axial ratio of the maximum cross section is to be taken as parameter from the family of curves.

The length l was taken not as the total length of the fuselage but as twice the distance from the nose to the position of maximum thickness, that is, as the length of the ellipsoid whose forward half forms this forward part of the fuselage.

The rearward position x of the neutral point of the friction lift referred to the $l/4$-point follows in accord with the definition of the coefficients as

$$\frac{x_n}{l} = \frac{dc_{m_{remainder}}}{dc_a} \frac{V^{1/3}}{l}$$

where

$$c_{m_{remainder}} = c_{m_{theoretical}} - c_{m_{experimental}}$$

The maximum increase of speed at the body is computed from the measured pressures as

$$\frac{v_{max}}{v_o} = \sqrt{\frac{p_o - p_{min}}{q} + 1}$$

RESULTS

The force measurements at fuselages 1 to 8 are reproduced in figure 2. They show the usual departure of the lift from linearity with the angle of attack and the instability of the fuselage moments. No breakaway of flow was observed throughout the employed angle-of-attack range. On fuselage 1 - D/L = 10 percent - it is noticed that stabilization results at $\alpha = 16^{\circ}$.

The effects of thickness ratio, rearward position of maximum thickness, and nose radius are represented in figures 3, 4, and 5.

The lift decreases toward greater D/L at all angles of attack, the drag increases with decreasing slenderness ratio, the test for D/L = 17.5 percent indicates a maximum value. The pitching moment is nearly constant. At $\alpha > = 16^{\circ}$ the moment of fuselage 1 - D/L = 10 percent - decreases substantially.

The rearward position of the maximum thickness has no effect on the lift with rising percentage. A slight decrease is observed at $\alpha > 20^{\circ}$.

The drag shows a distinct decrease with increasing rearward position of maximum thickness. The reason for it lies probably in the backward displacement of the transition point of the boundary-layer flow.

At small angles the pitching-moment coefficient is little affected by the rearward position of maximum thickness, at greater angles of attack a positive extreme value occurs at 40 percent. At $\alpha = 20^{\circ}$ and 30° a decrease with the rearward position is observed.

The effect of the nose radius is small. The drag increases slightly with increasing nose radius. From $\alpha = 10^{\circ}$ on the pitching moment shows a slight increase.

Figure 6 indicates the relationship between the increase in frictional lift and the angle of attack for $\alpha = 0^{\circ}$.

An increase in D/L is accompanied by an almost linear drop from 0.00891 at D/L = 10 percent to 0.0062 at D/L = 25 percent.

Nose radius and rearward position of maximum thickness show little influence.

A comparison of the measured moments with those obtained by potential theory (reference 1) discloses the much lower unstable value of the measurement. As explained in references 1 and 2, this is a consequence of the far back applied frictional lift. The moment of the lift referred to the 1/4-point as moment reference point is obtained by forming the difference between the theoretical and the measured moments. The linearity of this moment difference with the measured lift (fig. 7) enables a neutral point to be indicated as a function of the chosen parameters (fig. 8).

The pressure-distribution data are reproduced in figures 9 to 16. Included for comparison with theory are the p/q curves for 1 to 3 and 7, as obtained by the method (reference 3) for computing the pressure distribution on ellipsoidal bodies and by the method of surface superposition (which is to be published in the near future). The calculation by reference 3 applies to ellipsoids, so that agreement in pressure distribution is to be approximately expected only in the forward part, while by the second method the parabolically tapered tail end is also taken into account. A comparison of the two calculations discloses only minor differences.

The diagrams indicate good agreement between theory and test, particularly on the pressure side. The increases of velocity on the suction side are slightly less on the forward part. Greater differences are disclosed at high angles of attack, the suction side in particular fails to follow the theoretical pressure rise. Agreement fails also for the tail ond (see fuselage 7).

The relationship between maximum increase of velocity, and the three parameters is seon in figures 17 and 18. Several extreme values which as intermediate points could not be taken from the measurement, were obtained by appropriate completion of the pressuro-distribution curve.

Increasing thickness ratio is, as known, accompanied by a rise in the increase of velocity, which at small angles of attack corresponds very well to the theoretical values (reference 3). At greater angles of attack the differences are considerable.

Backward displacement of thickness is followed by reduction in the increase in velocity.

In flow along the plane of measurement the effect of the nose radius is small at small angles, but the increase in velocity rises with increasing angle of attack as a consequence of the transitional curvature at the nose (especially on fuselage 6). For yawed flow of the test section the effect is, naturally, small.

In general, the highest increases of velocity occur in symmetrical flow of test sections as compared to those in yawed flow.

The fuselage with curved mean line shows no special characteristics.

Translated by J. Vanier
National Advisory Committee
for Aeronautics

REFERENCES

1. Vandrey: Abschätzung des Rumpfeinflusses auf das Längsmoment eines Flugzeuges. FB 1093.

2. Multhopp, H: Aerodynamics of the Fuselage. NACA TM No. 1036, 1941.

3. Maruhn, K: Druckverteilung auf den gleichförmig geradlinig-bewegten 3-achsigen Ellipsoidkörper. FB 1174.

4. Kawalki, K. H.: Theoretische Untersuchungen von Schnellflugprofilen, die aus Ellipsenprofilen entwickelt sind. FB 1224.

TABLE I

ORDINATES OF SPINDLE-SHAPED FUSELAGES

x in percent t	Fuselage 1 y in percent t	Fuselage 2 y in percent t	Fuselage 3 y in percent t	Fuselage 4 y in percent t	Fuselage 5 y in percent t	Fuselage 6 y in percent t	Fuselage 7 y in percent t	Fuselage 8 y in percent t	Mean line fuselage 9 y in percent t
0	0	0	0	0	0	0	0	0	0
1.25	1.2625	2.1750	3.1250	2.6250	1.9380	4.5650	3.9990	4.0000	0
2.50	1.7500	3.0625	4.3125	3.6250	2.7500	5.6500	5.0900	5.1000	0
5.00	2.4375	4.2500	6.0250	5.0500	3.8650	7.0100	6.5700	6.5800	0
7.50	2.9375	5.1125	7.2875	6.0500	4.6250	7.9500	7.6500	7.6700	0
10.00	3.3125	5.7625	8.2500	6.7500	5.2700	8.7500	8.5400	8.5600	0
20.00	4.3250	7.6125	10.8625	8.3400	7.0300	10.9400	10.8800	10.9200	0
30.00	4.8500	8.5000	12.1500	8.7500	8.0500	12.1500	12.1125	12.1250	0
40.00	5.0000	8.7500	12.5000	8.4400	8.5600	12.5000	12.5000	12.5000	0
50.00	4.8375	8.5000	12.0875	7.6900	8.7500	12.1250	12.1500	12.1250	.5000
60.00	4.3625	7.7375	11.0000	6.5600	8.5600	11.0625	11.0125	11.0750	1.5250
70.00	3.6625	6.4750	9.2500	5.2000	7.9400	9.2500	9.2375	9.3000	3.1250
80.00	2.6875	4.7500	6.7500	3.6400	6.6000	6.7250	6.2750	6.7250	5.1625
90.00	1.4000	2.5250	3.6000	1.8880	4.0150	3.5750	3.5625	3.5000	7.4500
95.00	.7250	1.2875	1.8250	.9630	2.3250	1.8125	1.8000	1.7500	8.6875
100.00	0	0	0	0	0	0	0	0	9.8125

TABLE II

VARIATION OF SPINDLE-SHAPE FUSELAGES

No.	D/L in percent	ξ_D in percent	ρ	Fuselage form
1	10	40	Normal	Axially symmetrical
2	17.5	40	Normal	Do.
3	25	40	Normal	Do.
4	17.5	30	Normal	Do.
5	17.5	50	Normal	Do.
6	25	40	3x normal	Do.
7	25	40	2x normal	Do.
8	25	40	2x normal	Curved mean line

TABLE III

VOLUME OF FUSELAGES

Fuselage	$V m^3$	$V^{2/3} m^2$	$V^{1/3} (m)$
1	0.002362	0.01774	
2	.006915	.03629	
3	.014425	.05940	
4	.006630	.03555	
5	.007830	.03942	0.197
6	.014527	.05955	
7	.014710	.06015	
8	.013475	.05660	

TABLE IV

POLARS OF FUSELAGES 1 to 4

α	Fuselage 1			Fuselage 2		
	c_a	c_w	c_m	c_a	c_w	c_m
-10	-0.1002	0.0254	-0.1298	-0.0808	0.0406	-0.1644
-5	-.0521	.0172	-.0601	-.0402	.0318	-.0844
-1	-.0097	.0147	-.0101	-.0078	.0278	-.0163
0	0	.0141	0	0	.0285	0
1	.0073	.0144	.0203	.0087	.0271	.0163
2	.0181	.0155	.0314	.0177	.0285	.0310
4	.0361	.0197	.0627	.0355	.0299	.0636
6	.0542	.0228	.0943	.0495	.0313	.0978
10	.0898	.0290	.1571	.0827	.0366	.1628
15	.1392	.0561	.2122	.1199	.0511	.2453
20	.2033	.1018	.2074	.1661	.0726	.3058
25	.2988	.1678	.1336	.2192	.1043	.3193
30	.4278	.2410	.0193	.2814	.1470	.3173

α	Fuselage 3			Fuselage 4		
	c_a	c_w	c_m	c_a	c_w	c_m
-10	-0.0672	0.0321	-0.1678	-0.0895	0.0495	-0.1586
-5	-.0369	.0264	-.0873	-.0444	.0418	-.0826
-1	-.0076	.0243	-.0171	-.0087	.0361	.0176
0	0	.0240	0	0	.0347	0
1	.0067	.0264	.0122	.0122	.0354	.0108
2	.0092	.0257	.0350	.0232	.0361	.0267
4	.0245	.0279	.0640	.0417	.0381	.0566
6	.0347	.0285	.1013	.0598	.0390	.0900
10	.0599	.0332	.1670	.0907	.0481	.1568
15	.0930	.0433	.2403	.1298	.0608	.2409
20	.1362	.0669	.2855	.1693	.0820	.3069
25	.1852	.0972	.3096	.2234	.1108	.3328
30	.2474	.1325	.3117	.2832	.1515	.3403

TABLE IVa

POLARS OF FUSELAGES 5 to 8

α	Fuselage 5			Fuselage 6		
	c_a	c_w	c_m	c_a	c_w	c_m
-10	-0.0680	0.0377	-0.1799	-0.0641	0.0400	-0.1718
-5	-.0390	.0306	-.0859	-.0304	.0336	-.0884
-1	-.0073	.0280	-.0172	-.0059	.0294	-.0180
0	0	.0263	0	0	.0286	0
1	.0127	.0280	.0144	.0056	.0290	.0179
2	.0267	.0280	.0301	.0120	.0294	.0374
4	.0323	.0300	.0590	.0236	.0303	.0742
6	.0534	.0319	.0878	.0350	.0328	.1109
10	.0840	.0373	.1564	.0583	.0395	.1835
15	.1214	.0502	.2355	.0947	.0502	.2590
20	.1609	.0733	.2876	.1380	.0698	.3080
25	.2099	.1031	.3085	.1988	.0954	.3415
30	.2624	.1411	.3135	.2458	.1326	.3540

α	Fuselage 7			Fuselage 8		
	c_a	c_w	c_m	c_a	c_w	c_m
-10	-0.0602	0.0374	-0.1705	-0.0800	0.0591	-0.1183
-5	-.0294	.0300	-.0866	-.0431	.0483	-.0355
-1	-.0066	.0270	-.0178	-.0090	.0397	.0288
0	0	.0265	0	-.0084	.0393	.0530
1	.0055	.0273	.0170	.0044	.0384	.0663
2	.0118	.0288	.0340	.0113	.0384	.0827
4	.0239	.0293	.0688	.0270	.0397	.1163
6	.0368	.0297	.1043	.0442	.0411	.1468
10	.0598	.0363	.1775	.0748	.0506	.2085
15	.0941	.0464	.2511	.1148	.0582	.2825
20	.1372	.0636	.2983	.1580	.0779	.3300
25	.1851	.0888	.3280	.2170	.1080	.3538
30	.2426	.1391	.3356	.2792	.1455	.3570

TABLE V

LIFT, DRAG, AND MOMENT COEFFICIENTS AS FUNCTIONS OF THE PARAMETERS

Parameter		Coefficients	Angle of attack α (deg)					
			0	2	6	10	20	30
Slenderness ratio D/L	10 percent	c_a		0.0181	0.0542	0.0898	0.2033	0.4278
	17.5 percent			.0177	.0495	.0827	.1661	.2814
	25 percent			.0092	.0347	.0599	.1362	.2474
	10 percent	c_w	0.0141	.0155	.0228	.0290	.1018	.2410
	17.5 percent		.0285	.0285	.0313	.0366	.0726	.1470
	25 percent		.0240	.0257	.0285	.0332	.0669	.1325
	10 percent	c_m		.0314	.0943	.1571	.2074	.0193
	17.5 percent			.0310	.0978	.1628	.3058	.3173
	25 percent			.0350	.1013	.1670	.2855	.3117
Percent thickness ξ_D	30 percent	c_a		.0232	.0594	.0907	.1693	.2832
	40 percent			.0177	.0495	.0827	.1661	.2814
	50 percent			.0195	.0534	.0840	.1609	.2624
	30 percent	c_w	.0347	.0361	.0390	.0481	.0820	.1515
	40 percent		.0285	.0285	.0313	.0366	.0726	.1470
	50 percent		.0263	.0280	.0319	.0378	.0738	.1411
	30 percent	c_m		.0267	.0900	.1568	.3069	.3403
	40 percent			.0310	.0978	.1628	.3058	.3173
	50 percent			.0301	.0878	.1564	.2876	.3135
Nose radius ρ	1x	c_a		.0092	.0347	.0593	.1362	.2474
	2x			.0118	.0368	.0598	.1372	.2426
	3x			.0120	.0350	.0583	.1380	.2458
	1x	c_w	.0240	.0257	.0285	.0332	.0669	.1325
	2x		.0265	.0288	.0297	.0363	.0636	.1391
	3x		.0286	.0294	.0328	.0385	.0698	.1326
	1x	c_m		.0350	.1013	.1670	.2855	.3117
	2x			.0340	.1043	.1775	.2983	.3356
	3x			.0374	.1109	.1835	.3080	.3540

TABLE VI

$\frac{dc_a}{d\alpha}$ AS FUNCTION OF THE PARAMETERS

D/L percent	c_a'
10	0.00894
17.5	.0077
25	.00635

ξD percent	c_a'
30	0.00845
40	.0077
50	.00813

ρ	c_a'
1x	0.00635
2x	.0057
3x	.00583

TABLE VII

DIFFERENCE MOMENTS WITH RESPECT TO LIFT AS FUNCTION OF THE PARAMETERS

Parameter	α	Fuselage 1		Fuselage 2		Fuselage 3	
		Δc_m	c_a	Δc_m	c_a	Δc_m	c_a
Slenderness ratio D/L	-10	-0.1722	-0.1002	-0.1126	-0.0808	-0.0724	-0.0672
	-5	-.0886	-.0521	-.0562	-.0402	-.0346	-.0369
	0	.0092	0	0	0	0	0
	2	.0413	.0181	.0255	.0177	.0140	.0092
	6	.1041	.0542	.0706	.0495	.0446	.0347
	10	.1633	.0898	.1142	.0827	.0732	.0599
	15	.2520	.1392	.1597	.1199	.1112	.0930
	20	.3867	.2033	.2149	.1661	.1655	.1362
	30	.7779	.4278	.3842	.2814	.2770	.2474

Parameter	α	Fuselage 4		Fuselage 2		Fuselage 5	
		Δc_m	c_a	Δc_m	c_a	Δc_m	c_a
Percent thickness ξD	-10	-0.0875	-0.0895	-0.1126	-0.0808	-0.1141	-0.0680
	-5	-.0424	-.0444	-.0562	-.0402	-.0635	-.0390
	0	0	0	0	0.0	0	0
	2	.0235	.0232	.0255	.0177	.0299	.0195
	6	.0596	.0598	.0706	.0495	.0908	.0534
	10	.0893	.0907	.1142	.0827	.1376	.0840
	15	.1191	.1298	.1597	.1199	.1945	.1214
	20	.1561	.1693	.2149	.1661	.2650	.1609
	30	.2834	.2832	.3842	.2814	.4310	.2624

TABLE VII - Concluded

DIFFERENCE MOMENTS WITH RESPECT TO LIFT - Concluded

Parameter	α	Fuselage 3		Fuselage 7		Fuselage 6	
		Δc_m	c_a	Δc_m	c_a	Δc_m	c_a
Nose radius ρ	-10	-0.0724	-0.0672	-0.0698	-0.0602	-0.0685	-0.0641
	-5	-.0346	-.0369	-.0354	-.0294	-.0336	-.0304
	0	0	0	0	0	0	0
	2	.0140	.0092	.0151	.0118	.0117	.0120
	6	.0446	.0347	.0418	.0368	.0352	.0350
	10	.0732	.0599	.0628	.0598	.0568	.0583
	15	.1112	.0930	.1005	.0941	.0926	.0947
	20	.1655	.1362	.1537	.1372	.1440	.1380
	30	.2770	.2474	.2731	.2426	.2547	.2458

TABLE VIII

NEUTRAL POINT POSITION OF THE FRICTIONAL LIFT

D/L percent	$\frac{x}{t}$
10	0.3038
17.5	.3362
25	.3338

ξ_D percent	$\frac{x}{t}$
30	0.2410
40	.3362
50	.4170

ρ	$\frac{x}{t}$
1x	0.3338
2x	.3370
3x	.3120

TABLE IX

INCREASE OF SPEED AS FUNCTION OF THE PARAMETERS AT

ANGLE OF YAW $\beta = 0^{\circ}$ AGAINST ANGLE OF ATTACK α

Parameter			$\alpha=0^{\circ}$	$\alpha=4^{\circ}$	$\alpha=10^{\circ}$	$\alpha=15^{\circ}$	$\alpha=20^{\circ}$	$\alpha=25^{\circ}$	$\alpha=30^{\circ}$
D/L	10 percent	Practical	1.030	1.041	1.068	1.095	1.131	1.182	1.229
	17.5 percent		1.058	1.068	1.087	1.136	1.200	1.264	1.333
	25 percent		1.110	1.122	1.138	1.166	1.225	1.285	1.341
	10 percent	Theoretical	1.029	1.036	1.065	1.110	1.17	1.245	1.318
	17.5 percent		1.071	1.074	1.101	1.140	1.190	1.251	1.315
	25 percent		1.110	1.112	1.139	1.170	1.211	1.260	1.320
ξ_D	30 percent	Practical	1.078	1.090	1.112	1.136	1.191	1.250	1.320
	40 percent		1.058	1.068	1.087	1.136	1.200	1.264	1.333
	50 percent		1.048	1.053	1.068	1.108	1.165	1.224	1.280
a	1x	Practical	1.110	1.122	1.138	1.166	1.225	1.285	1.341
	2x		1.094	1.100	1.121	1.175	1.245	1.324	1.402
	3x		1.104	1.113	1.182	1.271	1.350	1.430	1.518

TABLE X

INCREASE OF SPEED AS FUNCTION OF THE PARAMETERS AT

$\alpha = 0$ AGAINST ANGLE OF YAW β

Parameter			$\beta=0^\circ$	$\beta=4^\circ$	$\beta=10^\circ$	$\beta=15^\circ$	$\beta=20^\circ$	$\beta=25^\circ$	$\beta=30^\circ$
D/L	10 percent	Practical	1.030	1.040	1.068	1.105	1.154	1.219	1.281
	17.5 percent		1.058	1.062	1.086	1.122	1.175	1.224	1.289
	25 percent		1.110	1.113	1.140	1.174	1.217	1.265	1.326
	10 percent	Theo-retical	1.028	1.035	1.065	1.113	1.175	1.239	1.316
	17.5 percent		1.070	1.075	1.103	1.143	1.194	1.250	1.320
	25 percent		1.110	1.114	1.140	1.170	1.211	1.260	1.322
ξ_D	30 percent	Practical	1.078	1.086	1.113	1.145	1.200	1.250	1.311
	40 percent		1.058	1.062	1.086	1.122	1.175	1.224	1.289
	50 percent		1.048	1.052	1.086	1.130	1.190	1.252	1.328
α	1x	Practical	1.110	1.113	1.140	1.174	1.217	1.265	1.326
	2x		1.094	1.104	1.130	1.160	1.210	1.265	1.320
	3x		1.104	1.113	1.130	1.166	1.216	1.270	1.328

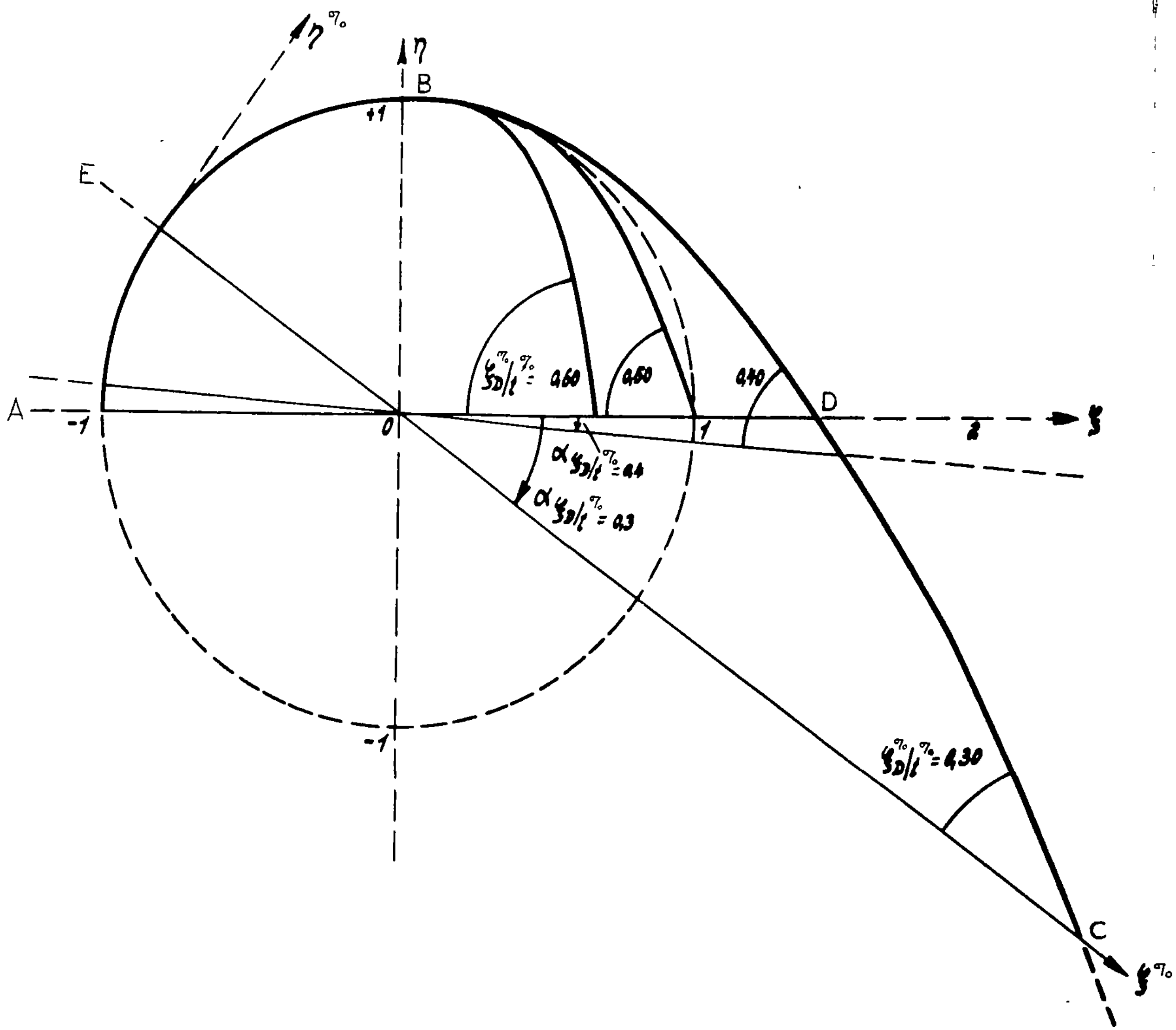

Figure 1a.- Basic profiles for different rearward positions of maximum thickness.

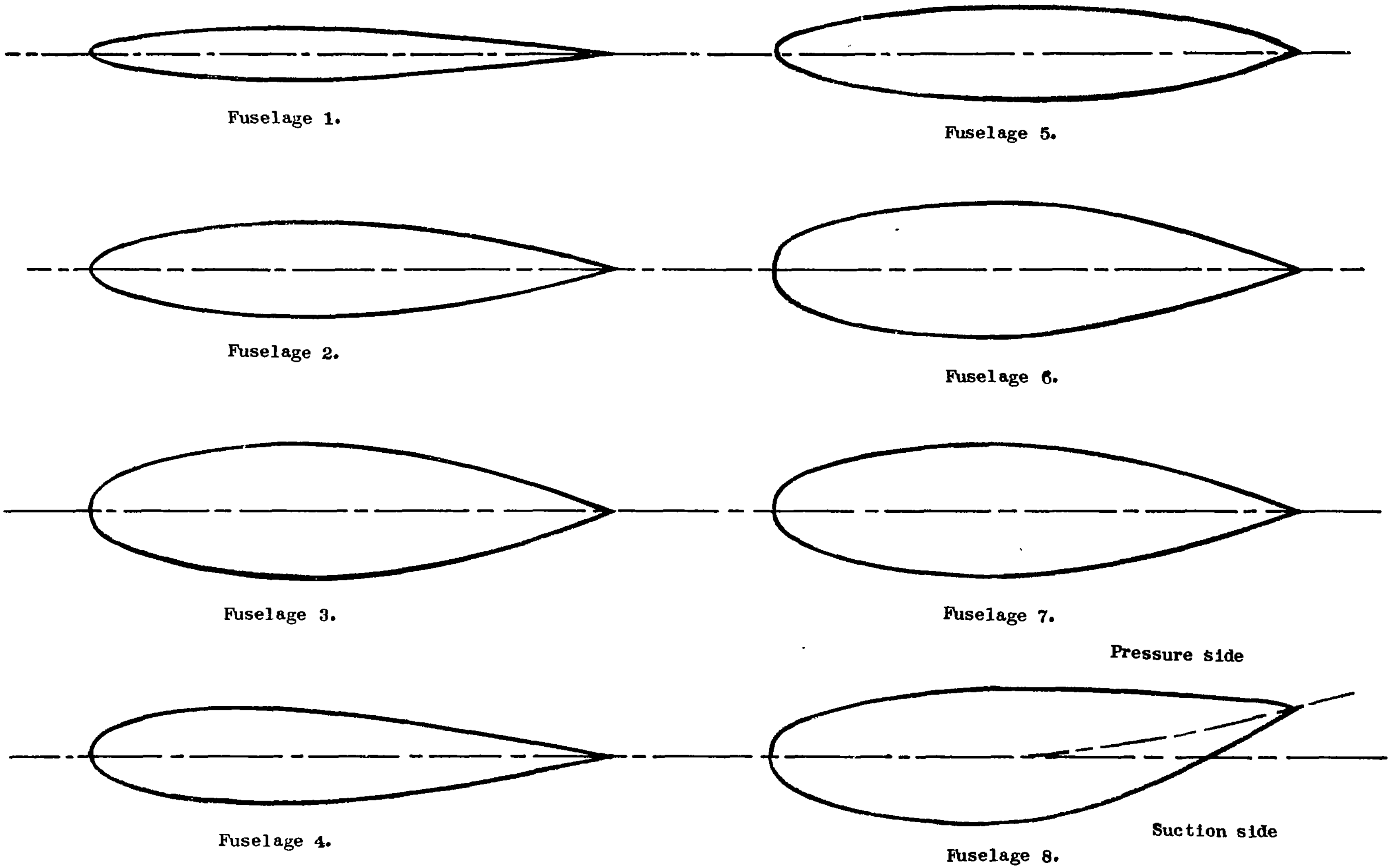

Figure 1b.- Experimental fuselage forms 1 to 8.

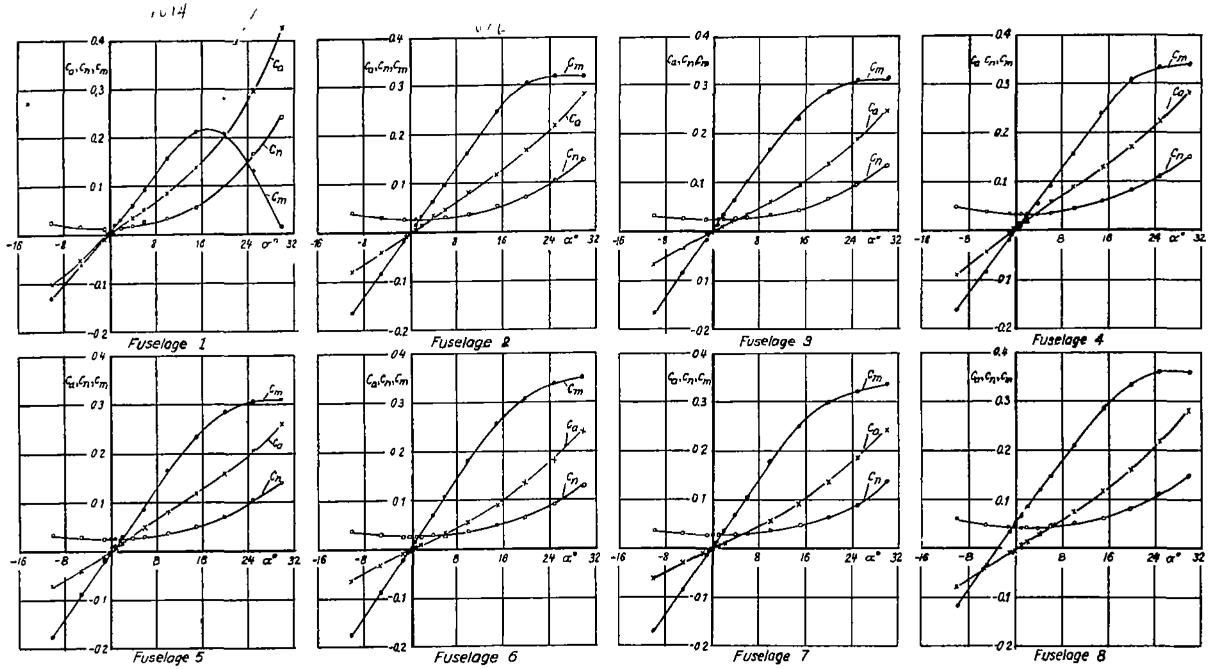

Figure 2.- Polars of force measurements for fuselages 1 to 8.

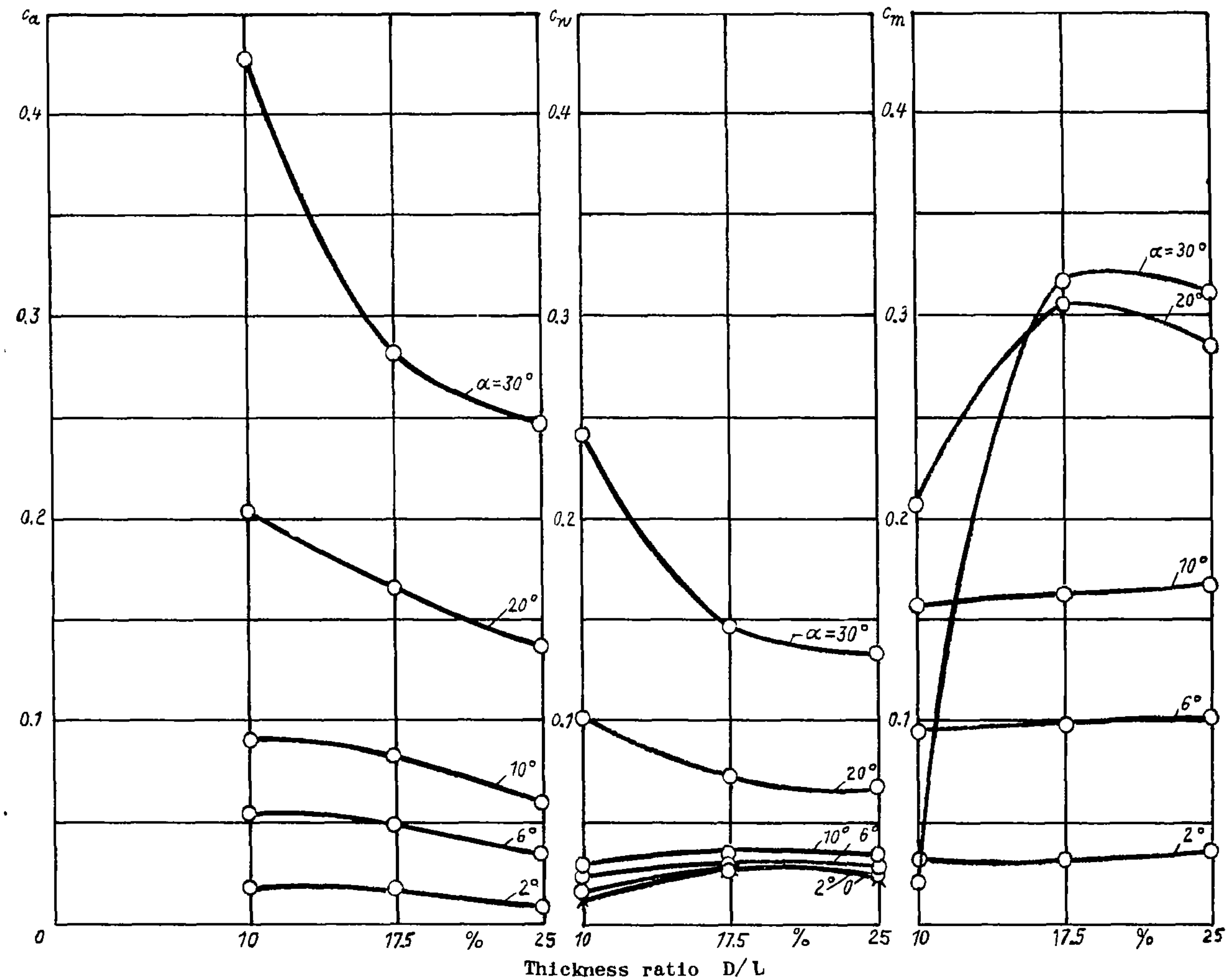

Figure 3.- Effect of $\frac{D}{L}$ on lift, drag, and pitching moment.

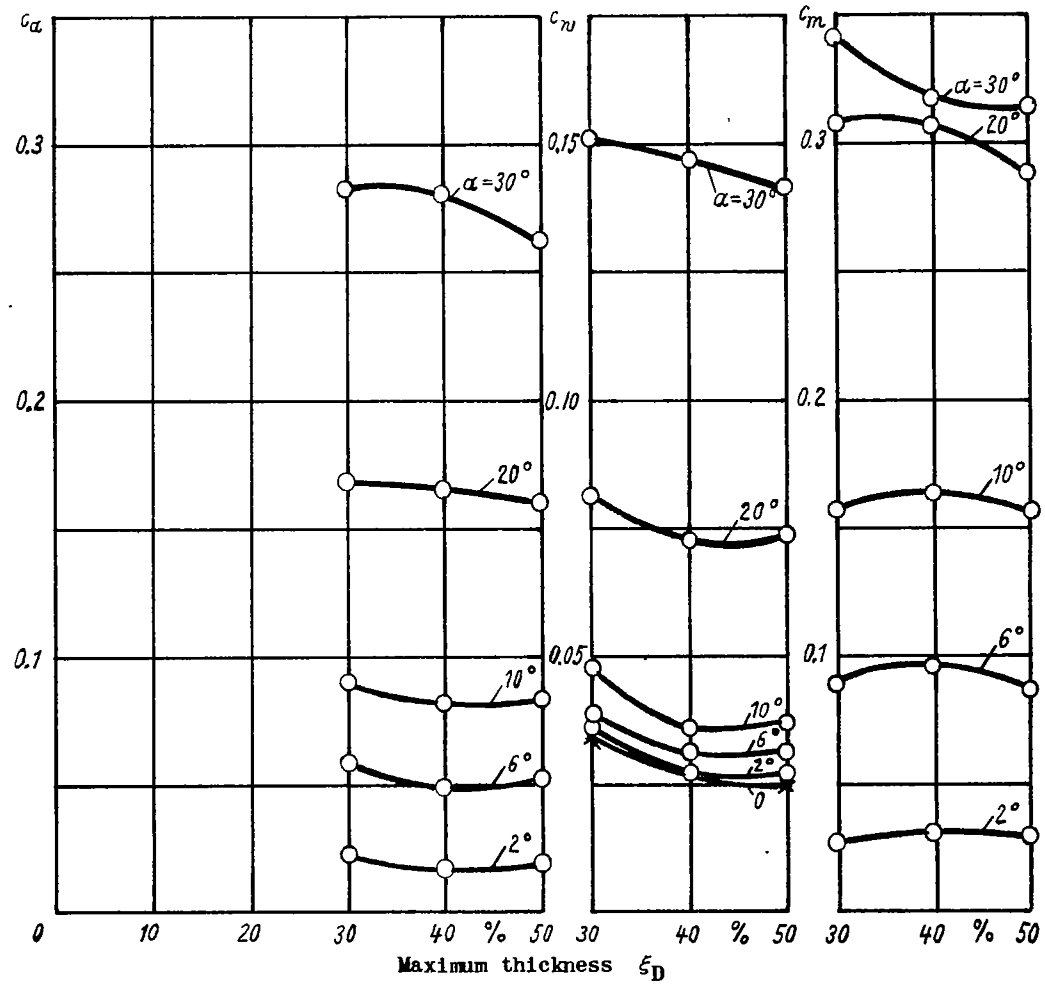

Figure 4.- Effect of ξ_D on lift, drag, and pitching moment.

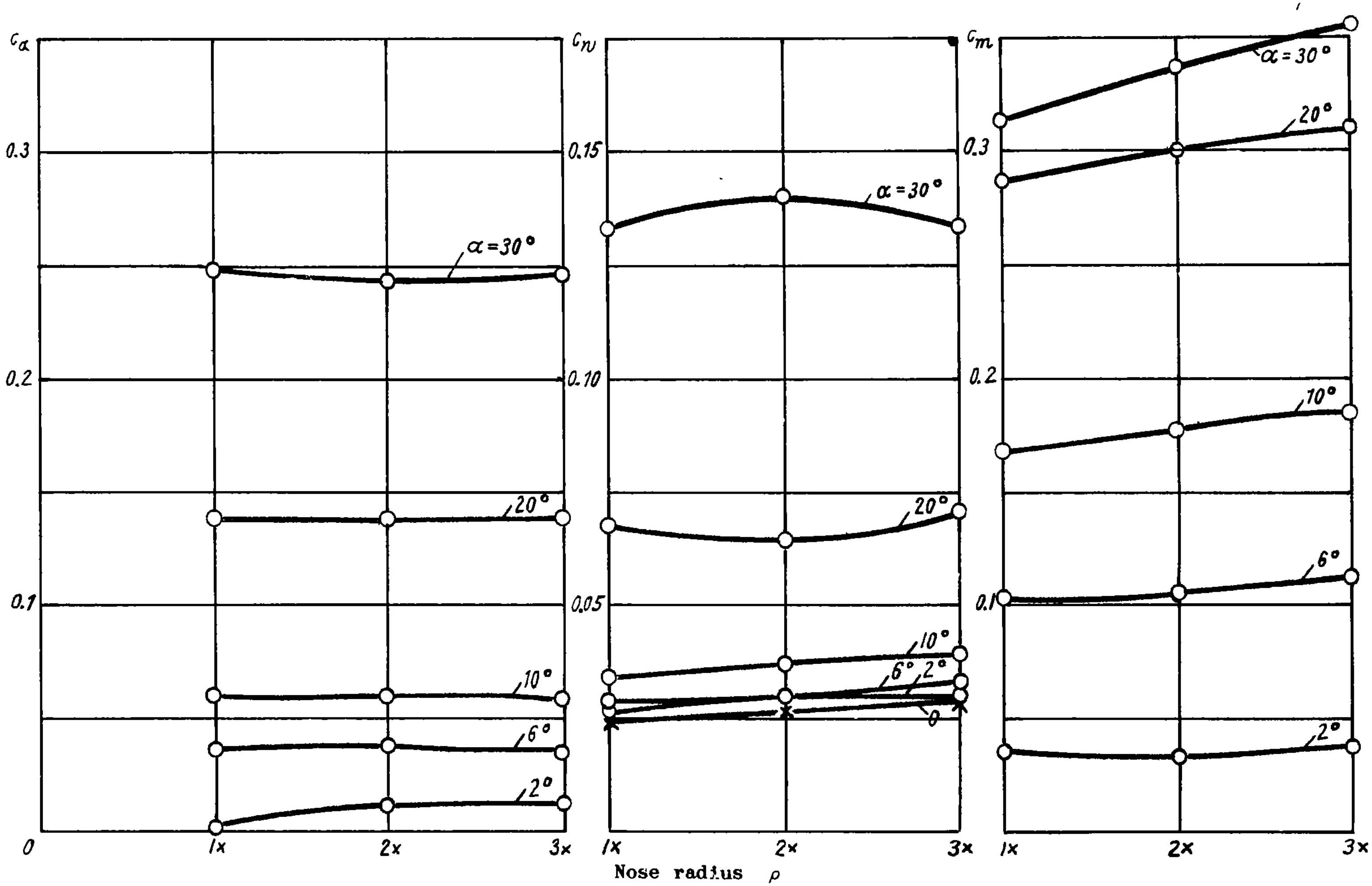

Figure 5.- Effect of nose radius ρ on lift, drag, and pitching moment.

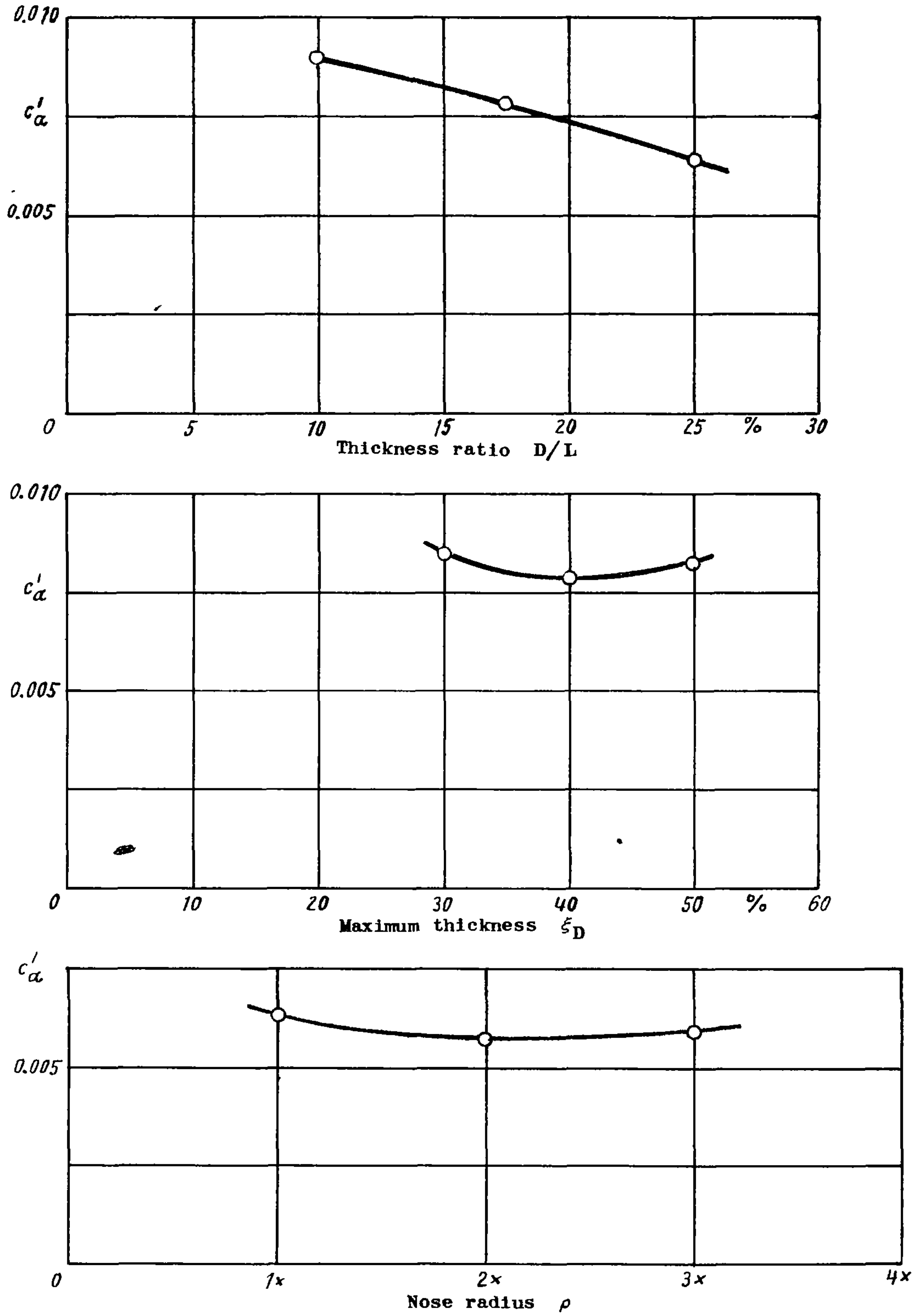

Figure 6.- Effect of $\frac{D}{L}$, ξ_D, and ρ on lift increase at $c_a' = 0^o$.

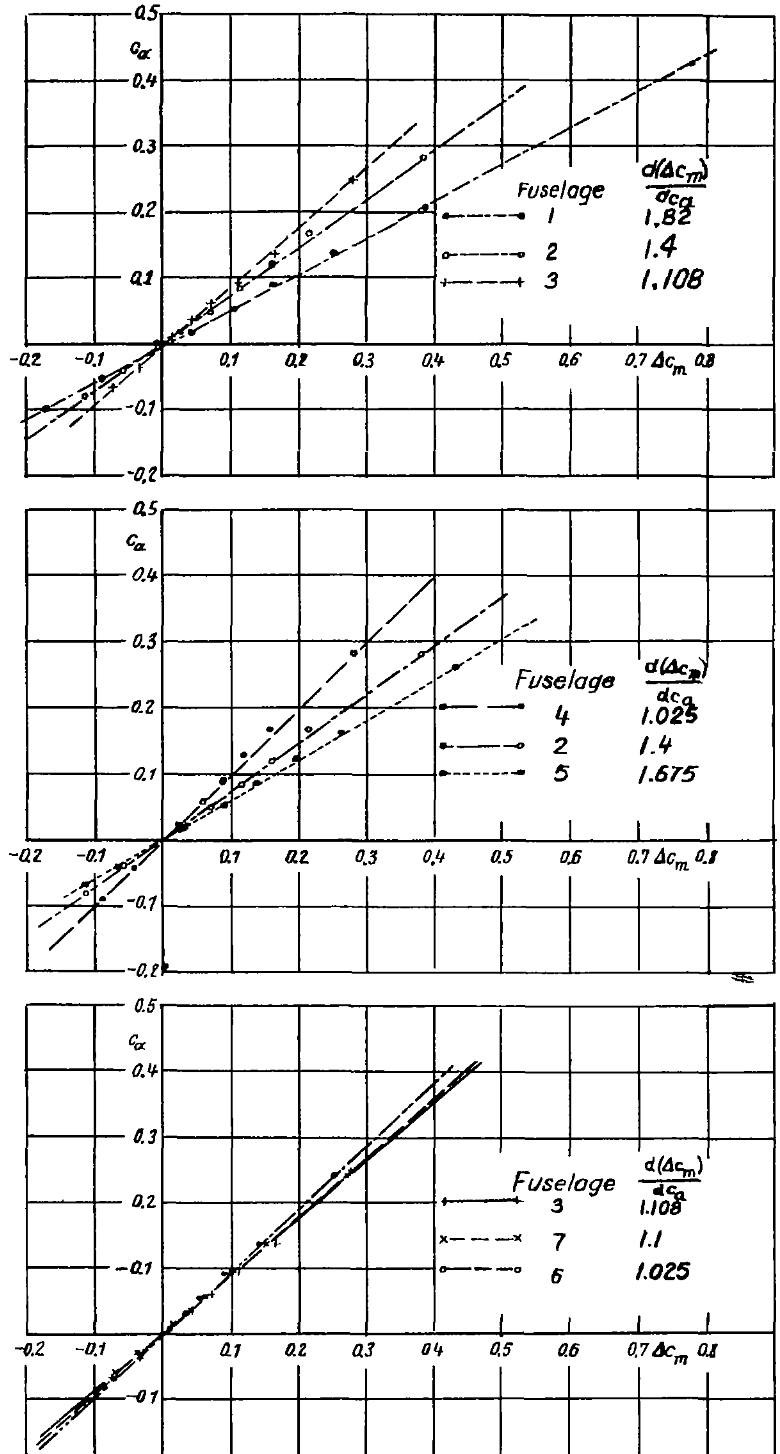

Figure 7.- Effect of $\frac{D}{L}$, ξ_D, and ρ on different moment relative to lift.

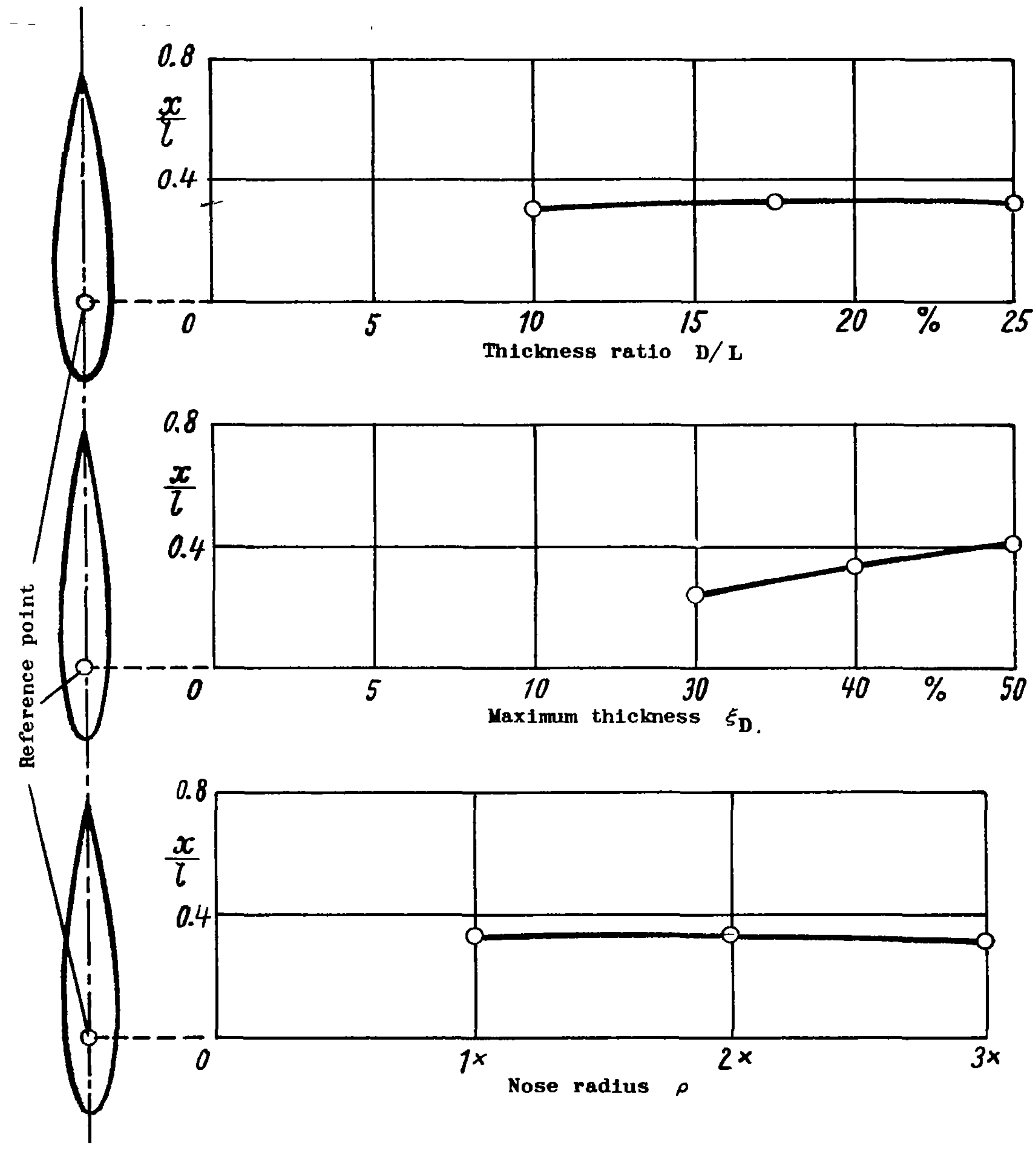

Figure 8.- Effect of $\frac{D}{L}$, ξ_D, and ρ on neutral point position of frictional lift.

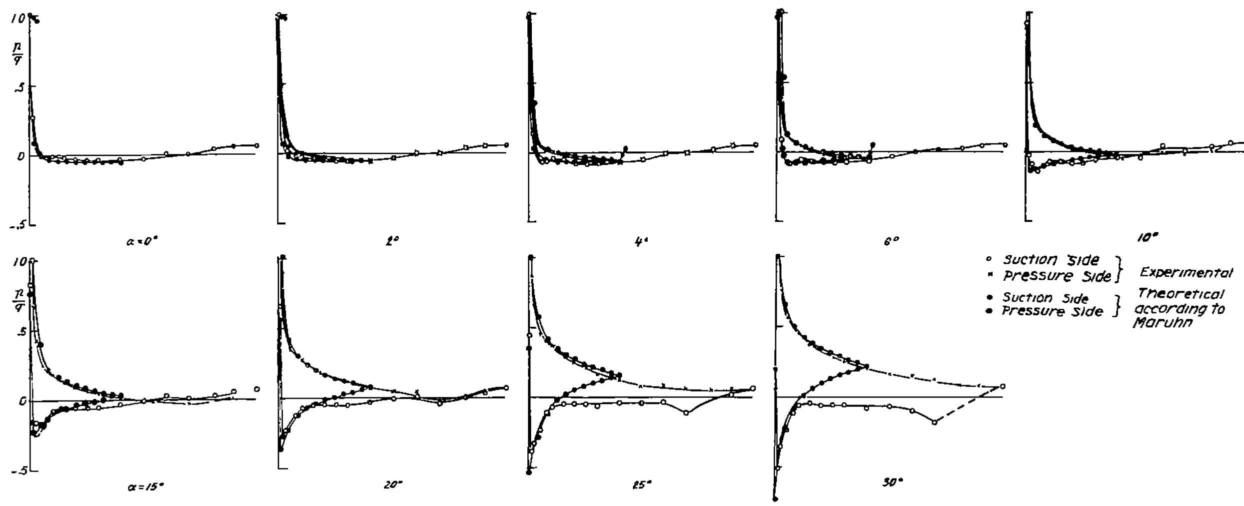

Figure 9.- Pressure-distribution record of fuselage 1 at $\beta = 0^{\circ}$ plotted against α.

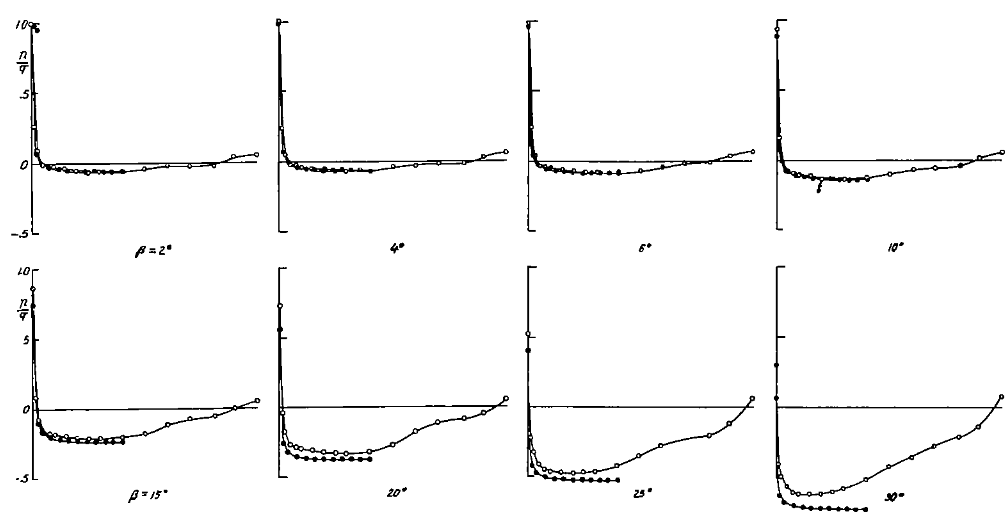

Figure 9a.- Pressure-distribution measurement of fuselage 1 at $\alpha = 0^{\circ}$ against β.

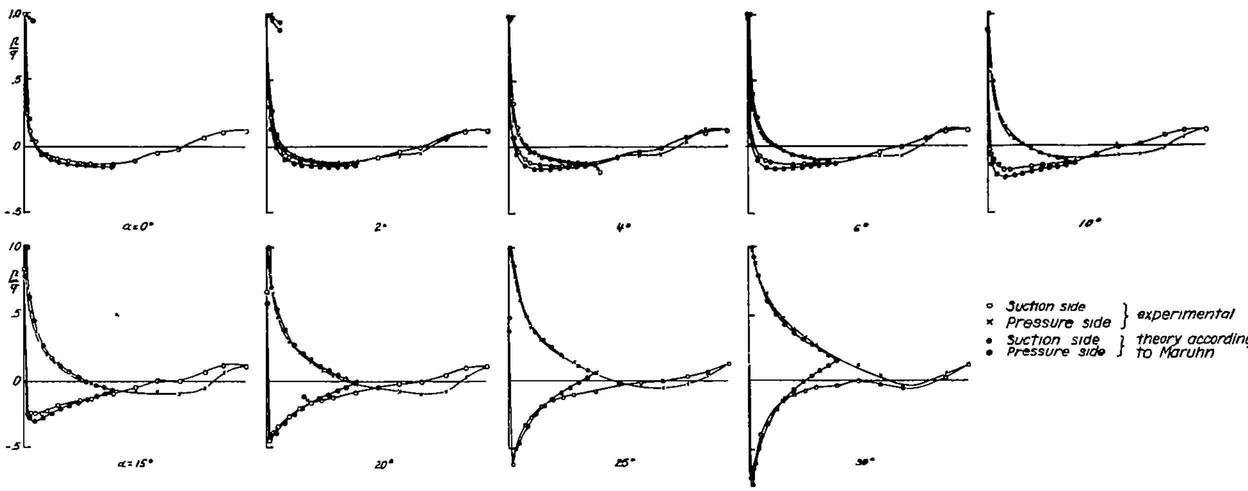

Figure 10.- Pressure-distribution record of fuselage 2 at $\beta = 0^{\circ}$ plotted against α.

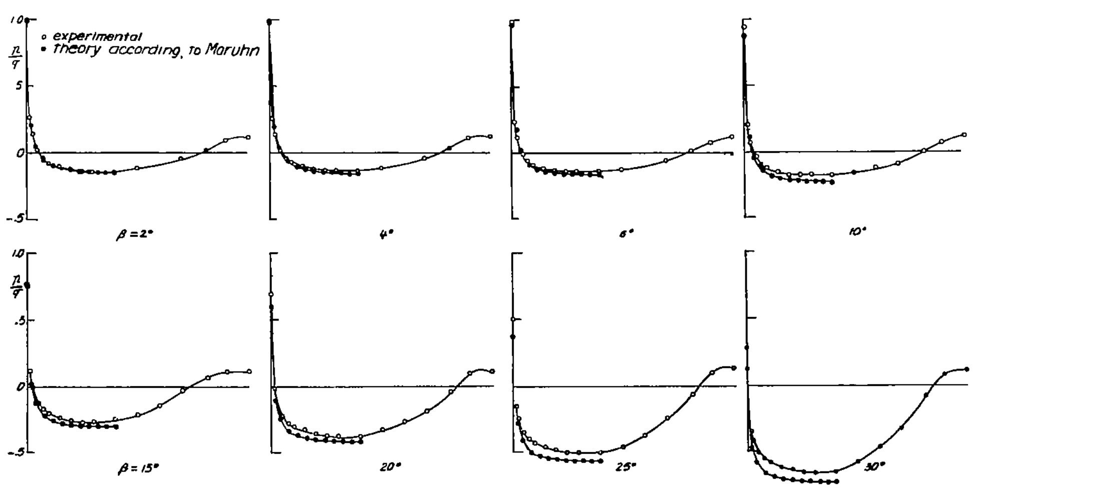

Figure 10a.- Pressure-distribution measurement of fuselage 2 at $\alpha = 0^{\circ}$ against β.

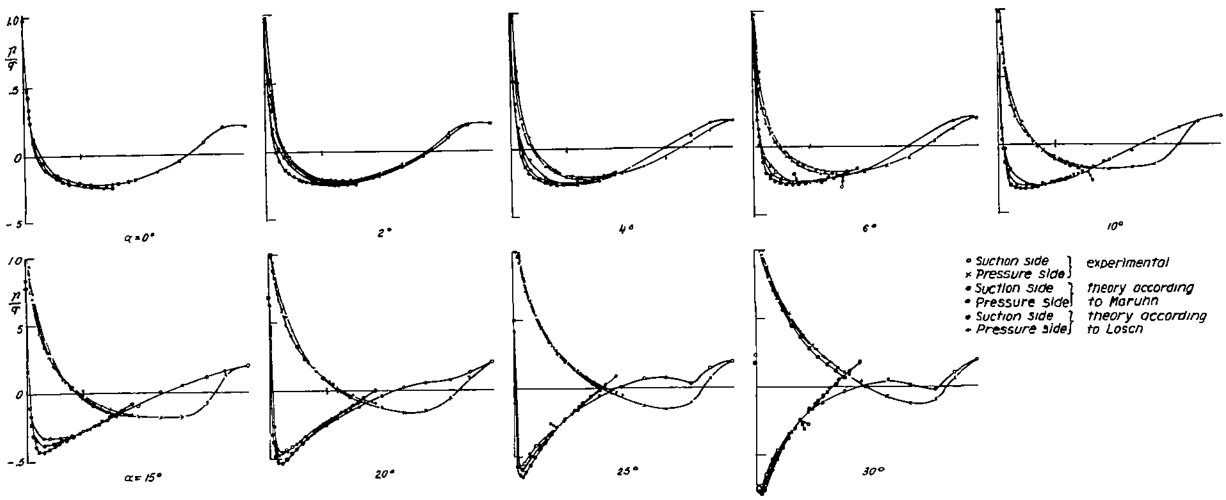

Figure 11.- Pressure-distribution measurement of fuselage 3 at $\beta = 0^{\circ}$ against α.

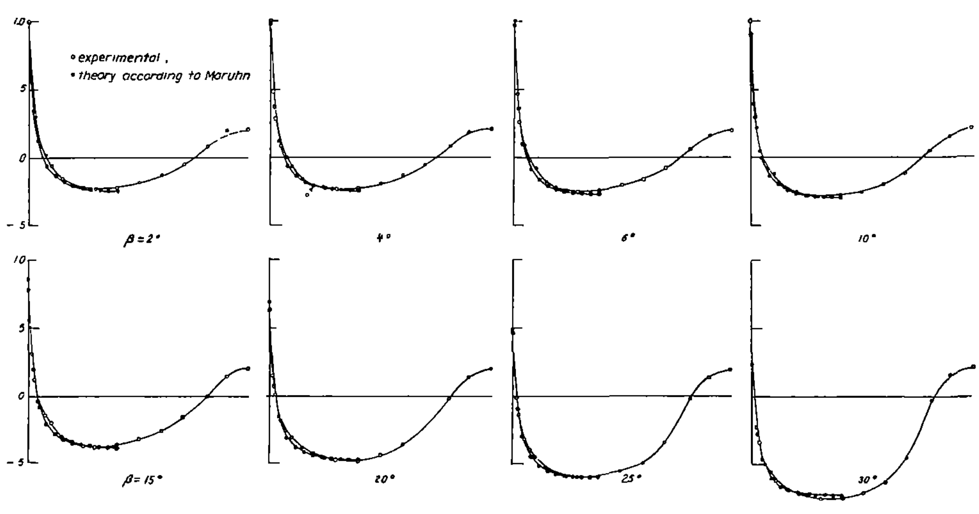

Figure 11a.- Pressure-distribution measurement of fuselage 3 at $\alpha = 0^{\circ}$ plotted against β.

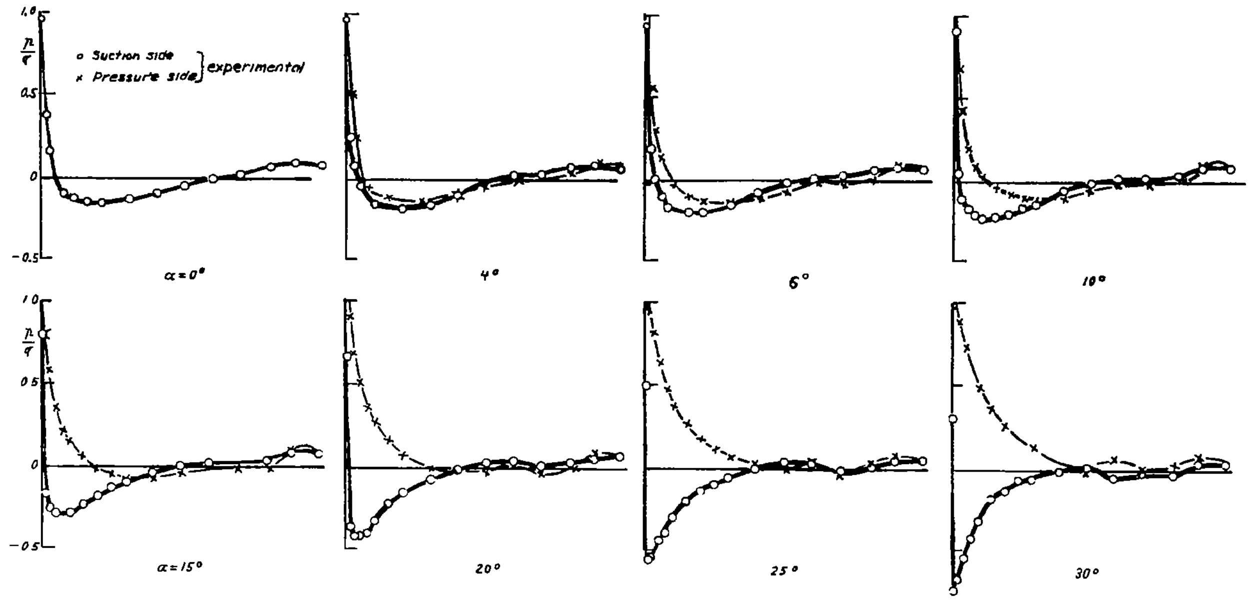

Figure 12.- Pressure-distribution measurement of fuselage 4 at $\beta = 0^{\circ}$ against α.

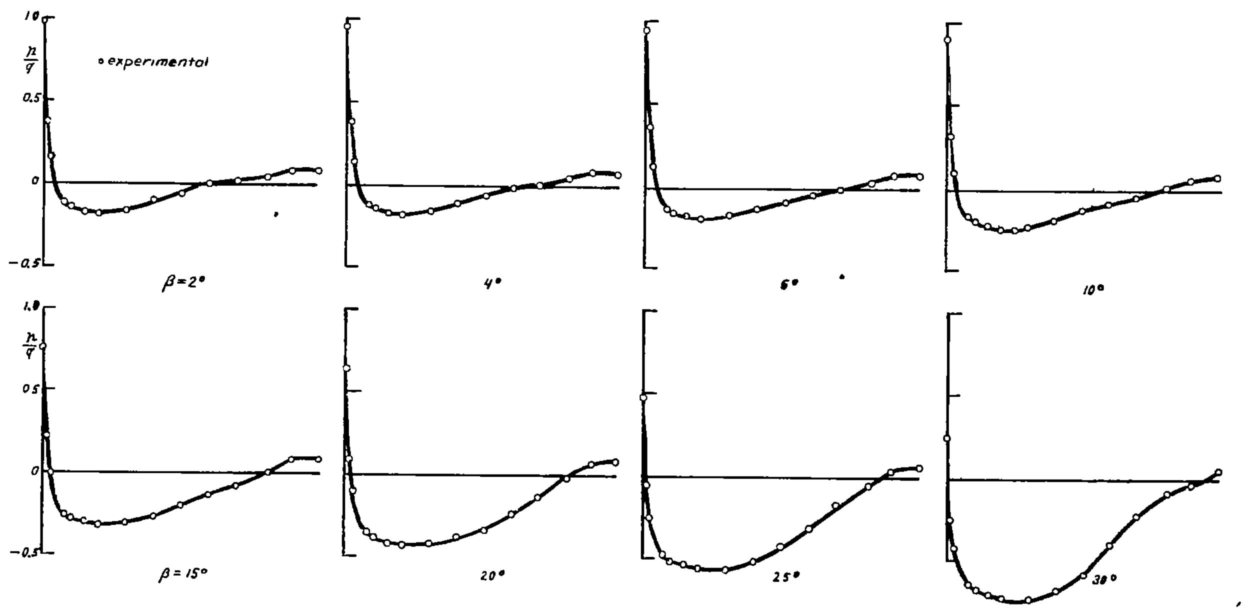

Figure 12a.- Pressure-distribution measurement of fuselage 4 at $\alpha = 0^{\circ}$ against β.

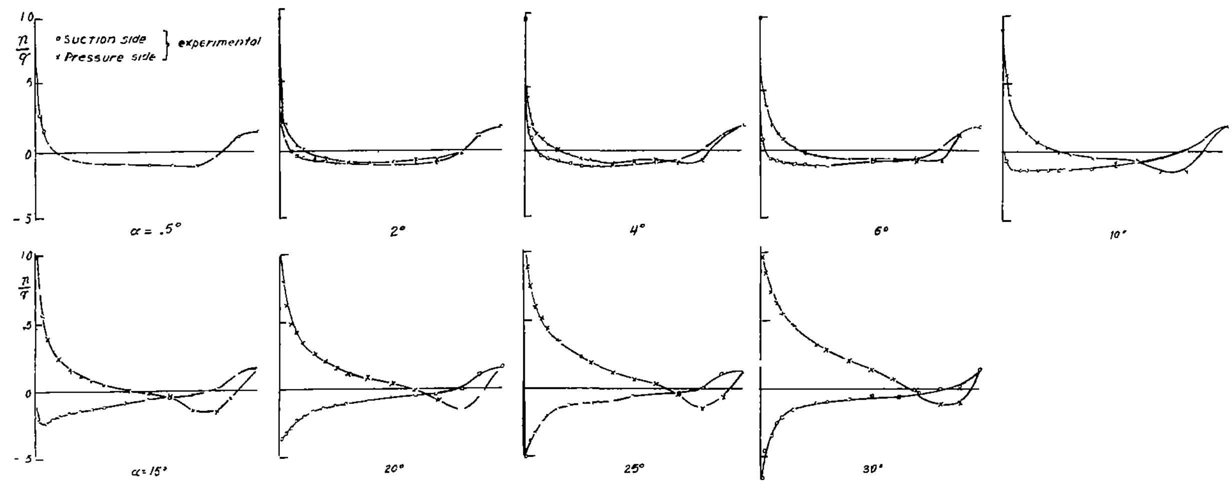

Figure 13.- Pressure-distribution measurement of fuselage 5 at $\beta = 0^{\circ}$ against α.

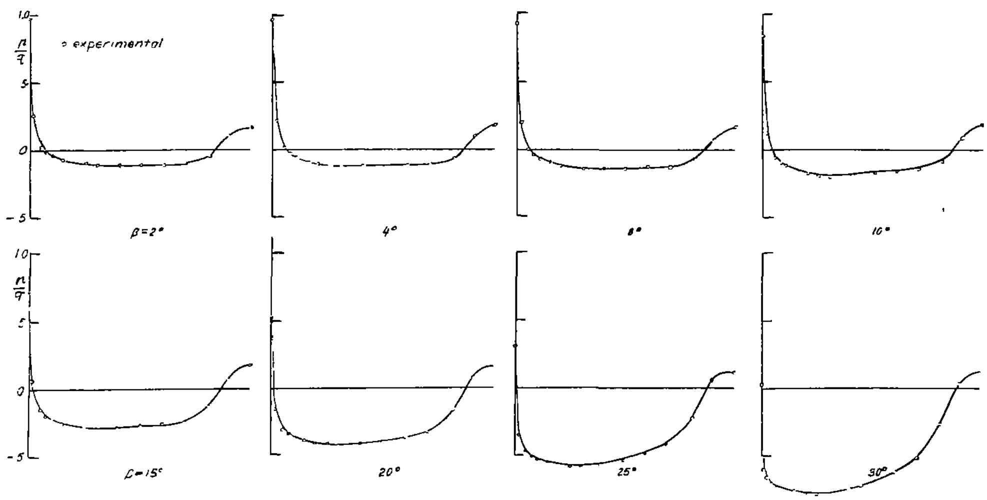

Figure 13a.- Pressure-distribution measurement of fuselage 5 at $\alpha = 0^{\circ}$ against β.

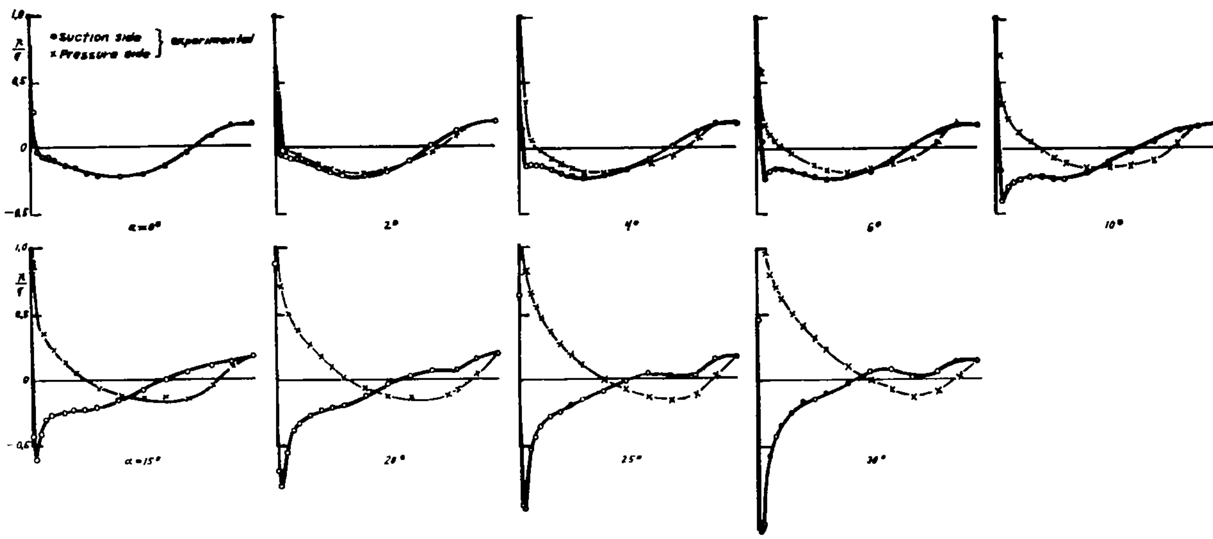

Figure 14.- Pressure-distribution measurement of fuselage 6 at $\beta = 0^{\circ}$ against α.

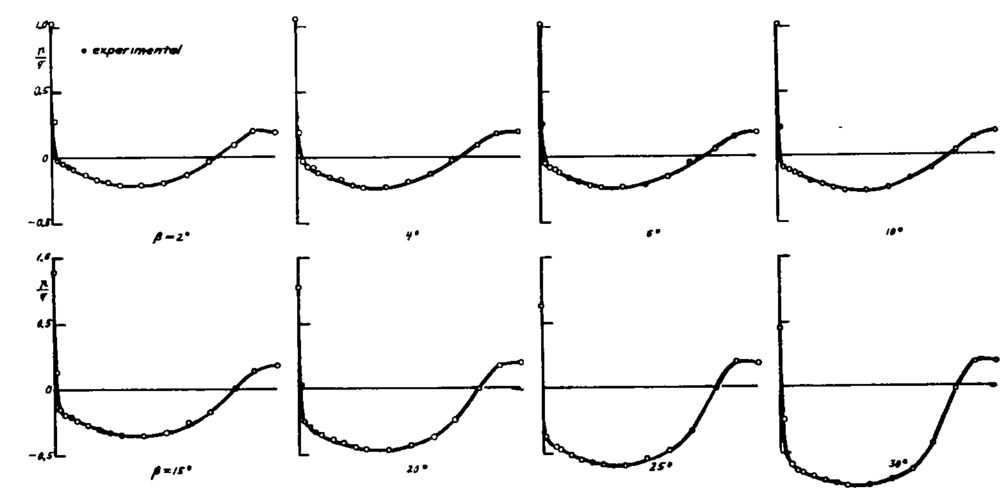

Figure 14a.- Pressure-distribution measurement of fuselage 6 at $\alpha = 0^{\circ}$ against β.

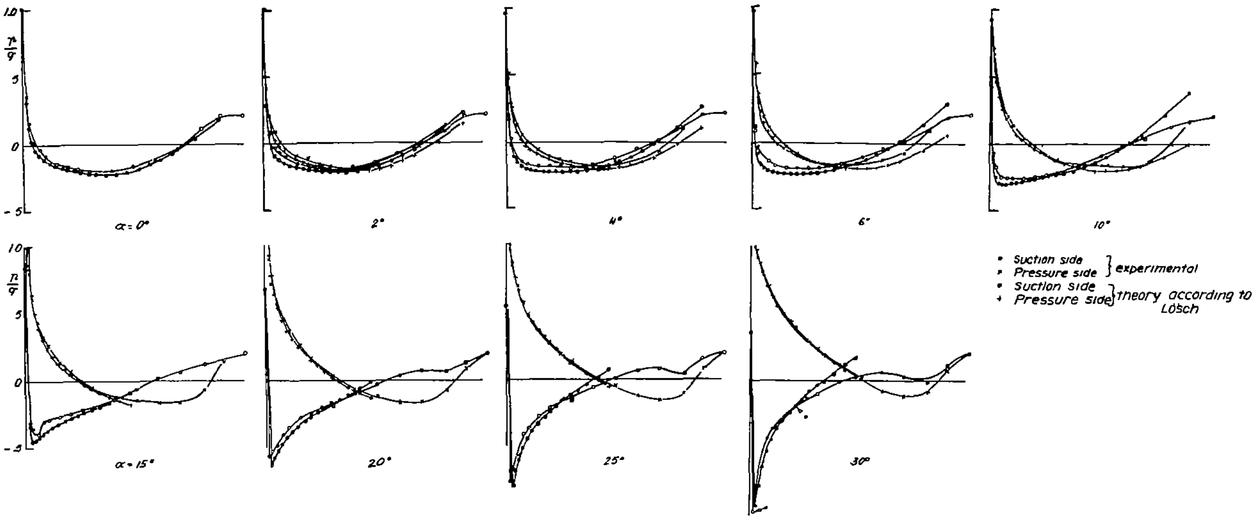

Figure 15.- Pressure-distribution measurement of fuselage 7 at $\beta = 0^{\circ}$ against α.

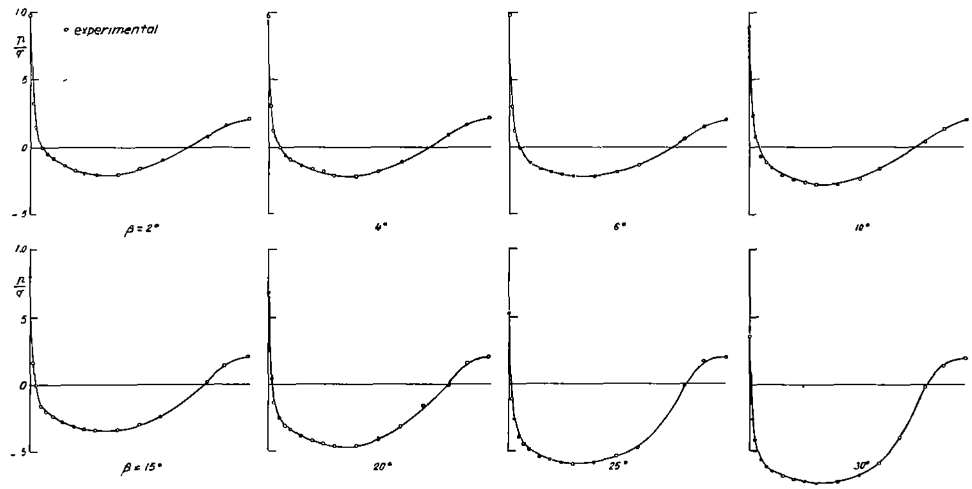

Figure 15a.- Pressure-distribution measurement of fuselage 7 at $\alpha = 0^{\circ}$ against β.

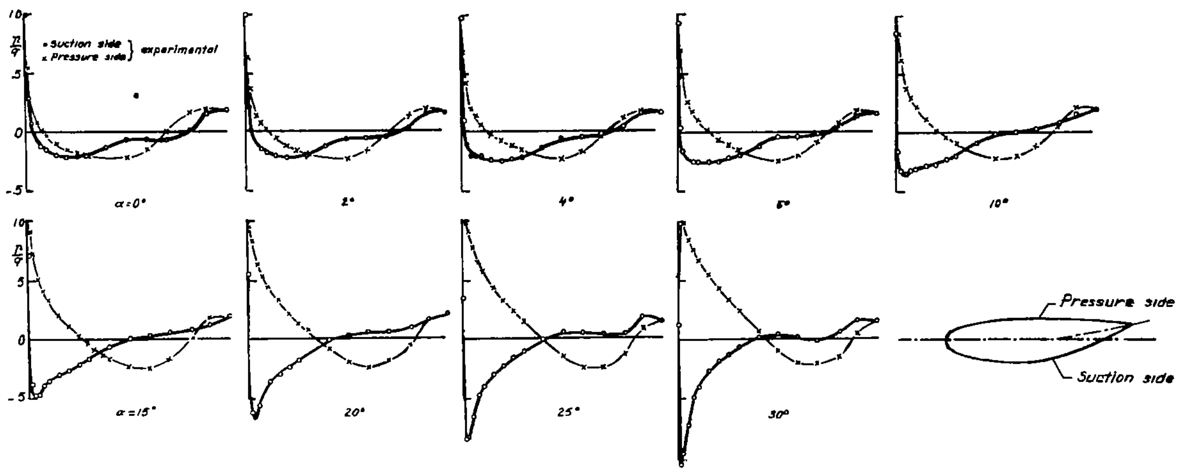

Figure 16.- Pressure-distribution measurement of fuselage 8 at $\beta = 0^\circ$ against α.

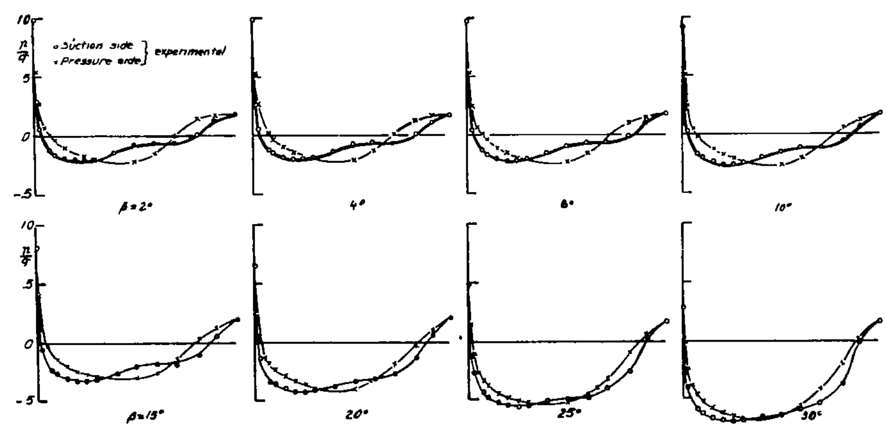

Figure 16a.- Pressure-distribution measurement of fuselage 8 at $\alpha = 0^\circ$ against β.

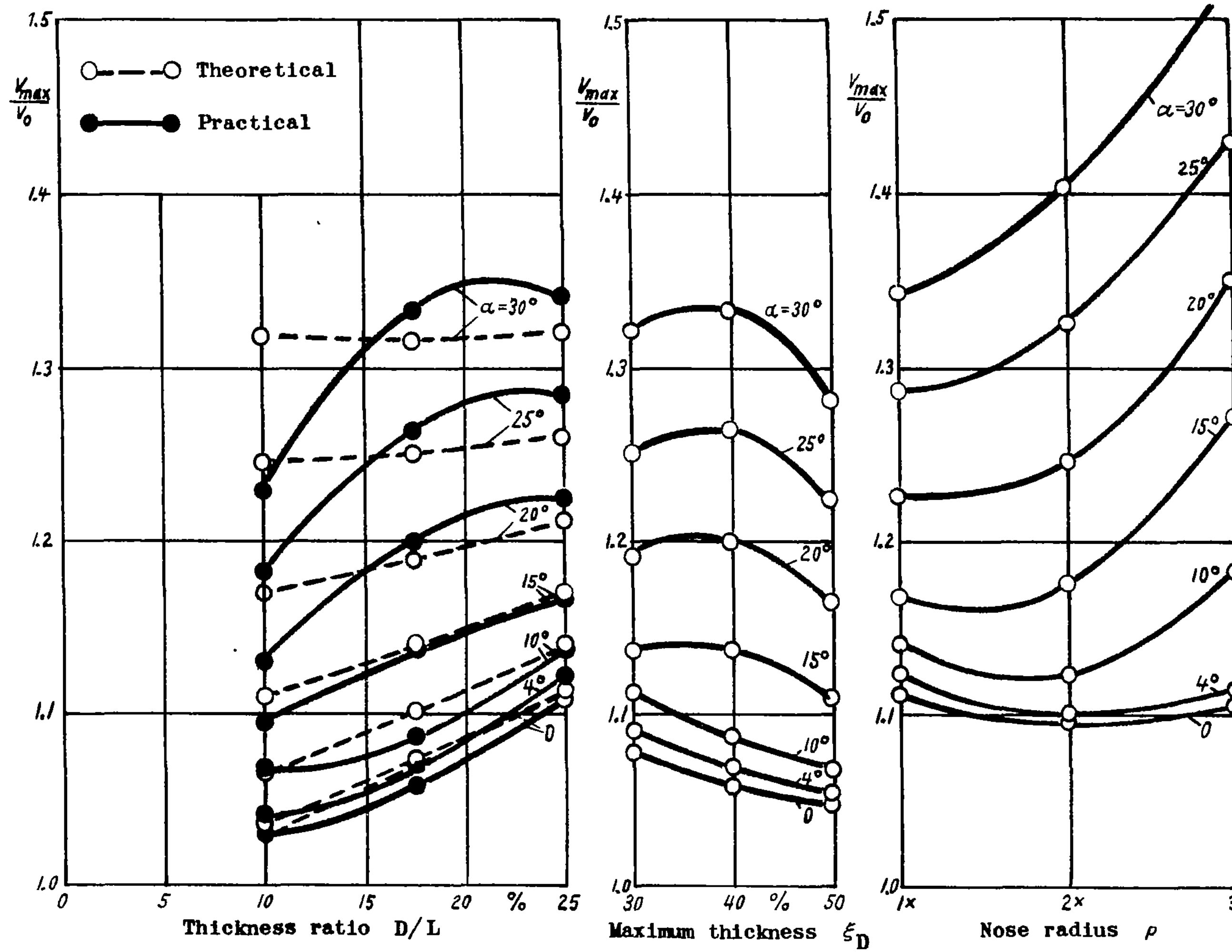

Figure 17.- Effect of $\frac{D}{L}$, ξ_D, and ρ on the maximum increase of speed at angle of yaw $\beta = 0$ plotted aginst angle of attack α.

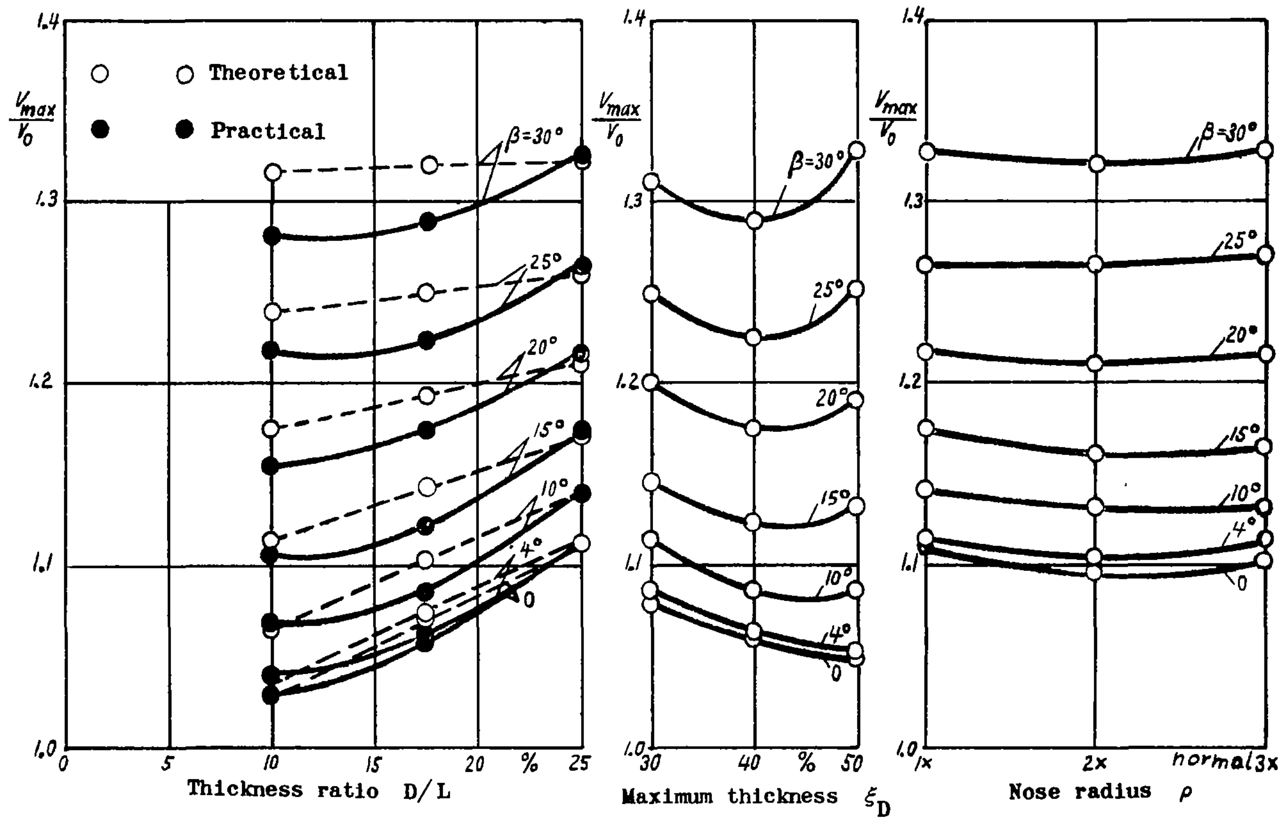

Figure 18.- Effect of $\frac{D}{L}$, ξ_D, and ρ on the maximum increase of speed at $\alpha = 0$ plotted against angle of yaw β.